JOURNAL OF SOLID STATE CHEMISTRY **133,** 156–159 (1997)
ARTICLE NO. SC977336

Electron Energy-Loss Spectroscopy Study of the Electronic Structure of α-Rhombohedral Boron

Masami Terauchi, Yosuke Kawamata, Michiyoshi Tanaka, Masatoshi Takeda,* and Kaoru Kimura*

*Research Institute for Scientific Measurements, Tohoku University, 2-1-1 Katahira Aoba-ku, Sendai 980, Japan; and *Department of Materials, The University of Tokyo, 7-3-1 Hongo, Bunkyo-ku, Tokyo 113, Japan*

Received January 30, 1997; accepted February 12, 1997

Electron energy-loss spectra of α-rhombohedral boron (α-r-B) were obtained from perfect crystalline areas of 180 nm diameter. The onset of the spectral intensity was observed at 2.4 eV (band gap energy). The volume plasmon peak due to the *sp* valence electrons is at 24.5 eV with a full width at half maximum of 7.5 eV. The real part $\varepsilon_1(\omega)$ and imaginary part $\varepsilon_2(\omega)$ of the dielectric function were obtained from the loss-function by Kramers–Kronig analysis. The value of $\varepsilon_1(0)$ was 6.5. $\varepsilon_2(\omega)$ showed clear peaks, not observed in $\varepsilon_2(\omega)$ of β-rhombohedral boron (β-r-B) and amorphous boron (am-B). K-shell excitation spectra show several peaks, which are not observed in the spectra of β-r-B and am-B. The characteristic structure of the peaks showed good agreement with a recent *ab initio* calculation within the local density approximation.

INTRODUCTION

Boron forms four allotropes: α-rhombohedral boron (α-r-B), α-tetragonal boron, β-rhombohedral boron (β-r-B), and β-tetragonal boron. These allotropes and amorphous boron (am-B) are constructed by B_{12} icosahedral clusters (1–3). The crystal structure of α-r-B is the simplest among them, in which B_{12} clusters are placed at the corners of the rhombohedral unit cell (4, 5). Each B_{12} cluster in α-r-B is covalently bonded to 12 nearest-neighbor B_{12} clusters. The B_{12} clusters in the (111) plane are connected by the three-center bonding and those between two (111) planes by the two-center bonding.

Theoretical calculations of the electronic structure of α-r-B indicate that α-r-B is a semiconductor with an indirect energy gap (6–8). Horn measured the band gap energy to be about 2 eV from optical absorption experiments of α-r-B single crystals (11). Domashevskaya *et al.* measured the density of states of the valence band of α-r-B, β-r-B, and am-B using X ray emission spectroscopy, but could not find a significant difference among them (12). Werheitet *et al.* conducted optical absorption experiments between 0.4 and 2.8 eV using powder specimens of α-r-B because the preparation of single crystals of α-r-B with a millimeter size was difficult (13). They found two interband transitions at 1.63 and 2.06 eV. To reveal the reliable electronic structure of α-r-B, experiments that can obtain spectra from small single crystalline areas over a wide energy range are needed. High-resolution electron energy-loss spectroscopy (EELS), which can select a microscopic area, is suitable for this purpose.

We acquired high-resolution EELS spectra from good single crystalline areas of α-r-B using a high-resolution EELS microscope (14, 15). We measured the band gap energy and volume plasmon energy. The dielectric function was derived from the loss-function by Kramers–Kronig analysis. We obtained B K-shell excitation spectra (B K-edge) of α-r-B and compared the spectra with a recent *ab initio* calculation within the local density approximation (16, 17). The spectra and dielectric functions of β-r-B and am-B, which were also obtained in the present study, are shown for comparison.

EXPERIMENTAL

Specimens of α-r-B were prepared by annealing am-B powder, which was prepared by electron-beam evaporation, at 1200°C for 10 h in a BN crucible. The crucible was held in an Ar-sealed quartz tube in which tantalum foil was set to prevent the specimens from oxidation. After annealing, the specimens were composed of small single crystals of α-r-B (20–40 μm) and β-r-B (50–100 μm). Electron diffraction patterns showed that the specimens examined were high quality single crystals of α-r-B. EELS spectra were obtained from specimen areas of 180 nm in diameter with a thickness of about 100 nm. The EELS microscope used was developed as a project of Joint Research with Industry by the Ministry of Education, Science, Sports, and Culture (14, 15). It is equipped with a thermal-type field emission gun as the electron source and specially designed double-focus Wien filters as the monochromator and analyzer. The illumination lens system, the specimen goniometer, and the imaging

0022-4596/97 $25.00

lens system of the EELS microscope are the same as the column part of a JEM1200EX transmission electron microscope. The EELS spectra were detected by a parallel-recording system with a charge-coupled device (CCD) camera. The best values of the full widths at half maximum (FWHM) of the zero-loss peak at present are 15 and 25 meV for the cases without and with a specimen, respectively. The accelerating voltage of incident electrons at the specimen was set at 60 keV. The retarding potential of the monochromator was set to be 51 V, and that of the analyzer to be 51–510 V.

RESULTS AND DISCUSSION

Figure 1 shows an electron microscope image of a piece of single crystalline α-r-B. A black circle shows a specimen area of 180 nm in diameter, from which EELS spectra were obtained. Figure 2 shows an EELS spectrum of α-r-B in an energy range of 1–40 eV together with spectra of β-r-B and am-B for comparison. Energy resolutions of these spectra were 0.18–0.19 eV. The steep decrease of spectral intensity around 1 eV is from the tail of the zero-loss peak. The energy onset of the spectrum of α-r-B is 2.4 eV (band gap energy), as indicated by an arrow. It is noted that the energy onset is larger than those of β-r-B (1.6 eV) and am-B (1.4 eV), which show good agreement with the values of 1.56 eV (β-r-B) (9) and 1.32 eV (am-B) (10), respectively, obtained by optical measurements. The value of α-r-B is larger by 0.4 eV than that of Horn (~2 eV) (11). Theoretical calculations indicated that the minimum indirect and the minimum direct interband transition energies are about 1.7 and 2.2–2.3 eV, respectively (6–8). Since the oscillator strength of the direct interband transition is larger than that of the indirect transition, the onset energy observed may be attributed to the minimum direct interband transition energy. The prominent peak observed at 24.5 eV (α-r-B) is due to the excitation of plasma oscillation of all valence electrons (volume plasmon). The value is close to 23.9 eV, which is calculated from the density of valence electrons, 4.12×10^{23} electrons/cm^3, under the assumption of the free electron model. It is noted that the value is nearly the same as those of β-r-B (24.0 eV) and am-B (24.2 eV) because the densities of valence electrons are similar among these three materials.

The single scattering spectrum was obtained by removing the contribution of the direct beam and the multiple inelastic scattering part using a Lorentz fit and the Fourier-log deconvolution method, respectively. The loss-function was obtained by applying the sum rule to the single scattering spectrum. The dielectric function was derived from the loss-function by Kramers–Kronig analysis (KKA). The integrations with energy in the sum rule and in the KKA were carried out up to 400 eV, where the intensity profiles above 60 eV were obtained by extrapolating the profiles using an E^{-3} dependence. Figure 3a shows the real part ε_1 and imaginary part ε_2 of the dielectric function of α-r-B in an energy range of 0–30 eV together with those of β-r-B and am-B for comparison. The condition for the plasmon excitation, $\varepsilon_1 = 0$, is satisfied at 23.3 eV (α-r-B), 23.0 eV (β-r-B), and 22.9 eV (am-B). This confirms the assumption that the

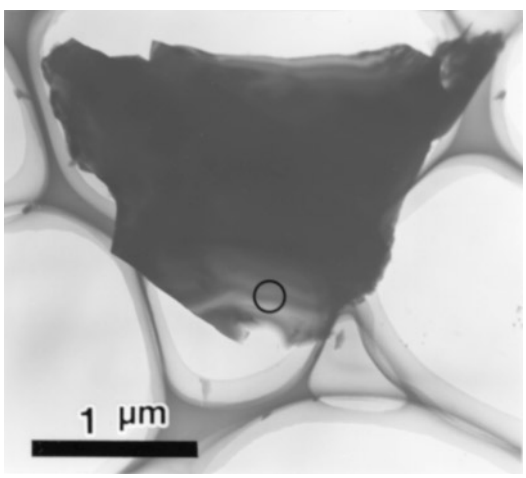

FIG. 1. Electron microscope image of a piece of single crystalline α-r-B. A black circle shows a specimen area of 180 nm in diameter, from which EELS spectra were obtained.

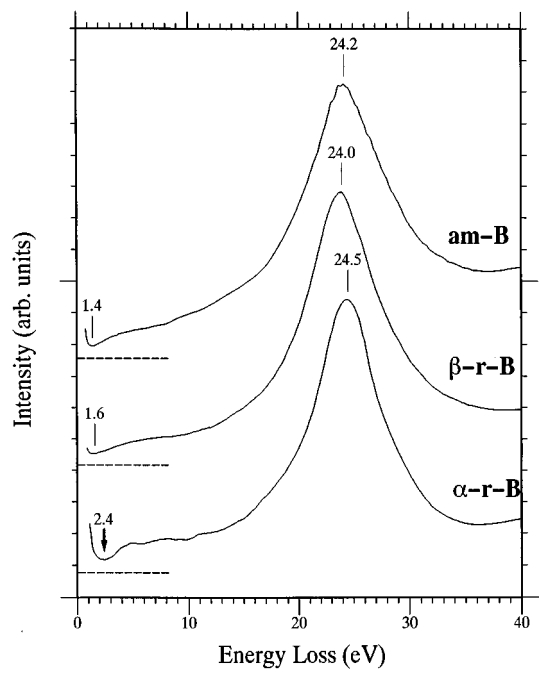

FIG. 2. Electron energy-loss spectrum of α-r-B in an energy range of 1–40 eV together with spectra of β-r-B and am-B for comparison. Energy resolutions were 0.18–0.19 eV.

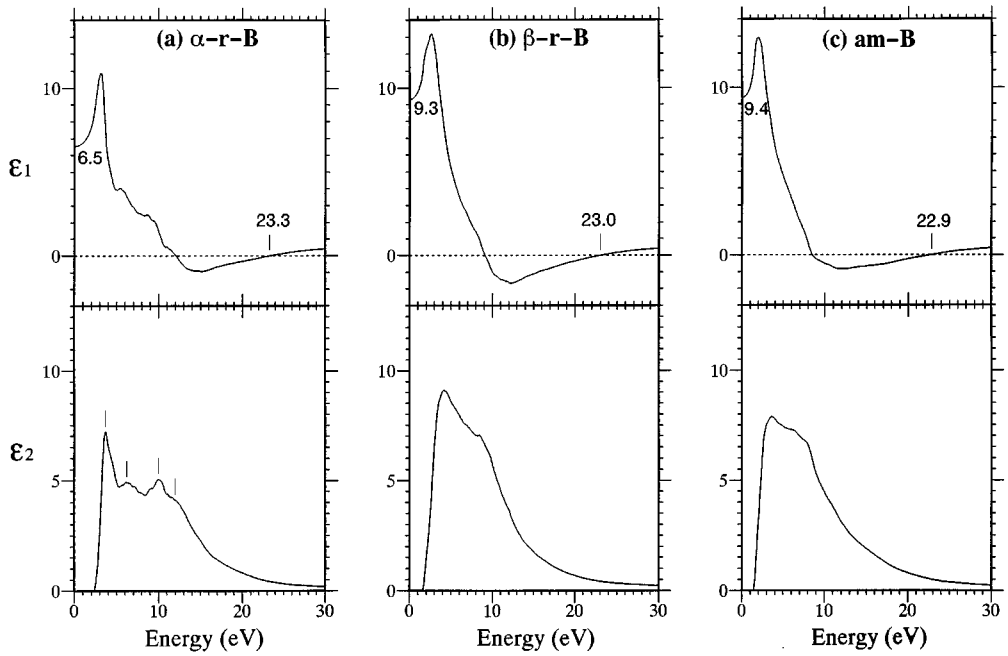

FIG. 3. Real part ε_1 and imaginary part ε_2 of the dielectric function of α-r-B in an energy range of 0–30 eV together with those of β-r-B and am-B for comparison.

peaks 24–25 eV in Fig. 2 correspond to the volume plasmon excitation. The FWHM value of the volume plasmon peak of α-r-B (*sp* semiconductor) is 7.5 eV, which is a little smaller than those of β-r-B (8.5 eV) and 10 eV (am-B). The value of α-r-B is about twice the value of *sp* semiconductors Si and Ge (~ 4 eV). The large FWHM value of α-r-B, which indicates a strong damping of the volume plasmon, is due to a large value of ε_2 at the energy of $\varepsilon_1 = 0$. The value of $\varepsilon_1(0)$ of α-r-B is 6.5, which is smaller than those of β-r-B (9.3 eV) and am-B (9.4 eV). The smaller $\varepsilon_1(0)$ value of α-r-B than those of β-r-B and am-B is explained by the larger band gap energy of α-r-B than those of β-r-B and am-B. ε_2 of α-r-B shows four peaks and/or shoulders (indicated by vertical lines) due to interband transitions, which were not observed in ε_2 of β-r-B and am-B. These peaks are considered to originate from the structure in the density of states of the conduction band and/or the valence band.

Figure 4a shows a B K-edge of α-r-B in an energy range of 185–205 eV together with spectra of β-r-B and am-B for comparison. Energy resolutions of the spectra were about 0.2 eV. The onset of the B K-edge of α-r-B was observed at 188.6 eV. The value of the onset energy is a little larger than those of β-r-B (187.8 eV) and am-B (187.4 eV). It can be attributed to the fact that the band gap energy of α-r-B is larger than those of β-r-B and am-B. The spectrum of α-r-B shows clear peaks which were not observed in the spectra of β-r-B and am-B. The peaks indicate that there is a peak structure in the density of states (DOS) of the conduction band of α-r-B. It may be an origin of the appearance of peaks and/or shoulders in the ε_2 in Fig. 3a. The appearance of the clear peaks in Fig. 4a may be attributed to the fact that all B_{12} clusters in α-r-B are deformed in the same manner, while four different types of deformation of B_{12} clusters occur in β-r-B (18). The superposition of four different types of spectra may smear out the clear peaks originated from one deformation in the case of β-r-B. The intensity profile of B K-edge from am-B and β-r-B are similar. This similarity indicates that the basic structures of am-B and β-r-B are the same, which is consistent with the analysis of the radial distribution functions of boron allotropes by Kobayashi (3). Figure 4b shows the B K-edge of α-r-B and the DOS of the conduction band of α-r-B obtained by Gunji (16) using an *ab initio* calculation within the local density approximation (17). The peak positions in the B K-edge of α-r-B show good agreement with those in the calculated density of states. Gunji assigned the peaks A and B to the B2*s*–2*p* hybridized states and the B2*p* states, respectively. The experimental peak intensity at 189.6 eV appears much smaller than that in the calculated density of states. Since the B K-edge was obtained under the condition of dipole transition, the partial density of states with *p* character in unoccupied states was observed. Thus, the experimental peak intensity at 189.6 eV should be smaller than that in the calculated density of states, which include states with *s* character. The present study successfully revealed the electronic structure of α-r-B by taking the electron energy-loss spectra from high-quality single crystals of α-r-B with high energy resolutions.

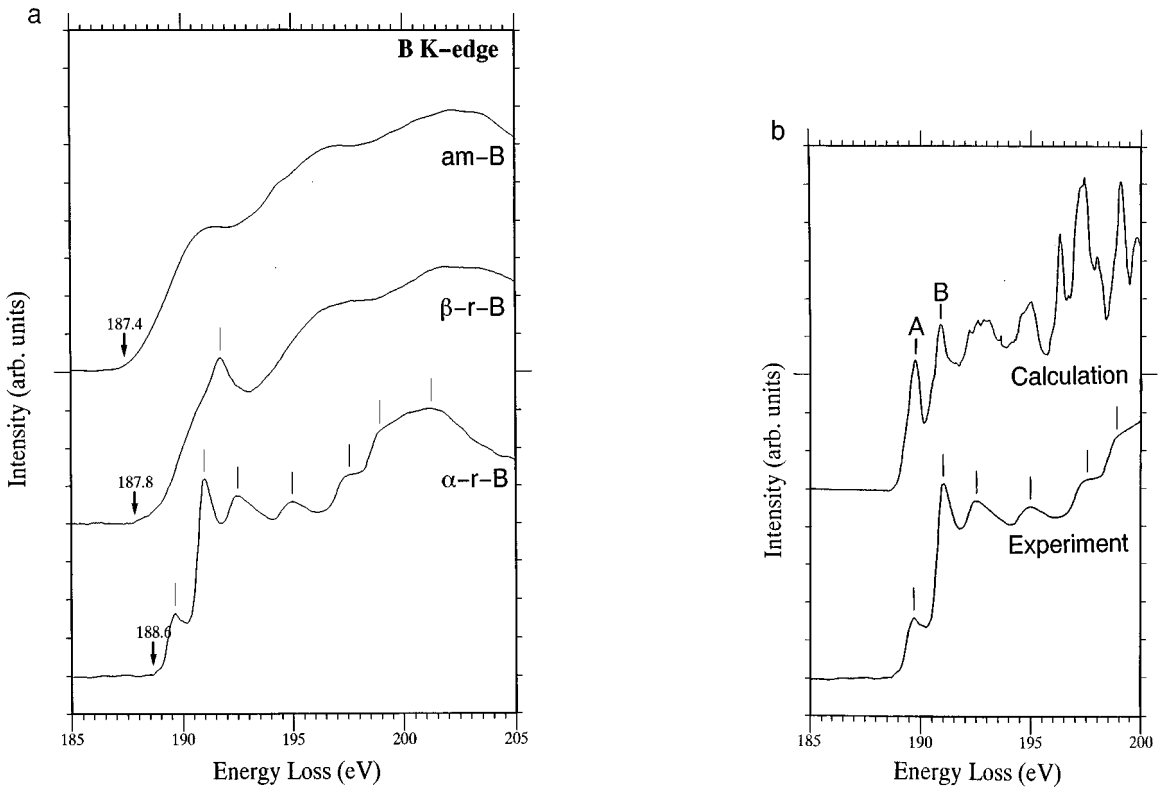

FIG. 4. (a) B K-shell excitation spectrum (B K-edge) of α-r-B in an energy range of 185–205 eV together with spectra of β-r-B and am-B for comparison. Energy resolutions for the spectra were about 0.2 eV. (b) B K-edge of α-r-B and the density of states of the conduction band of α-r-B obtained by an *ab initio* calculation within the local density approximation (16, 17).

ACKNOWLEDGMENTS

The authors thank Dr. Y. Harada, Mr. M. Ishida, Dr. K. Tsuno and Mr. M. Kai of JEOL Ltd. for their great effort in constructing the high-resolution EELS microscope. They thank Mr. F. Sato for his skillful technical assistance. The present work was partly supported by a Grant-in-Aid from the Ministry of Education, Science, Sports and Culture, Japan.

REFERENCES

1. O. A. Golicova, *Phys. Stat. Sol.* **101,** 277 (1987).
2. K. Katada, *Jpn. J. Appl. Phys.* **5,** 582 (1966).
3. M. Kobayashi, *J. Mater. Sci.* **23,** 4392 (1988).
4. L. V. McCarty, J. S. Kasper, F. H. Horn, B. F. Decker, and A. E. Newkirk, *J. Am. Chem. Soc.* **80,** 4507 (1958).
5. B. F. Decker and J. S. Kasper, *Acta Crystallogr.* **12,** 503 (1959).
6. D. W. Bullett, *J. Phys. C* **15,** 415 (1982).
7. S. Lee, D. M. Bylander, and L. Kleinman, *Phys. Rev. B* **42,** 1316 (1990).
8. D. Li, Y. N. Xu, and W. Y. Ching, *Phys. Rev. B* **45,** 5896 (1992).
9. R. Franz and H. Werheit, *AIP Conf. Proc.* **231,** 29 (1991).
10. C. Feldman, F. Ordway, W. Zimmerman III, and K. Moorjani, "Boron," Vol. 2, p. 235. Plenum, New York, 1965.
11. F. H. Horn, *J. Appl. Phys.* **30,** 1611 (1959).
12. E. P. Domashevskaya, N. E. Solovjev, V. A. Terekhov, and Ya. A. Ugai, *J. Less-Common Metals* **47,** 189 (1976).
13. H. Werheitet, U. Kuhlman, N. E. Solov'ev, G. P. Tsiskarishvili, and G. Tsagareishvili, *AIP Conf. Proc.* **231,** 350 (1991).
14. M. Terauchi, R. Kuzuo, F. Satoh, M. Tanaka, K. Tsuno, and J. Ohyama, *Microsc. Microanal. Microstruct.* **2,** 351 (1991).
15. M. Tanaka, M. Terauchi, R. Kuzuo, K. Tsuno, J. Ohyama, and Y. Harada, "Proceedings, 50th Annual Meeting of Electron Microscopy Society of America," p. 940, 1992.
16. S. Gunji, Doctor thesis, Science Univ. of Tokyo, 1995.
17. S. Gunji and H. Kamimura, *Jpn. J. Appl. Phys. Series* **10,** 35 (1994).
18. M. Fujimori and K. Kimura, *J. Solid State Chem.* **133,** 178 (1997).